PNAS RESEARCH ARTICLE | EVOLUTION OPEN ACCESS

Preserved soft anatomy confirms shoulder-powered upstroke of early theropod flyers, reveals enhanced early pygostylian upstroke, and explains early sternum loss

Michael Pittman[a,1], Thomas G. Kaye[b], Xiaoli Wang[c,1], Xiaoting Zheng[c,d], T. Alexander Dececchi[e], and Scott A. Hartman[f]

Edited by Dennis Voeten, Uppsala University; received March 29, 2022; accepted September 29, 2022 by Editorial Board Member Scott V. Edwards

Anatomy of the first flying feathered dinosaurs, modern birds and crocodylians, proposes an ancestral flight system divided between shoulder and chest muscles, before the upstroke muscles migrated beneath the body. This ancestral flight system featured the dorsally positioned deltoids and supracoracoideus controlling the upstroke and the chest-bound pectoralis controlling the downstroke. Preserved soft anatomy is needed to contextualize the origin of the modern flight system, but this has remained elusive. Here we reveal the soft anatomy of the earliest theropod flyers preserved as residual skin chemistry covering the body and delimiting its margins. These data provide preserved soft anatomy that independently validate the ancestral theropod flight system. The heavily constructed shoulder and more weakly constructed chest in the early pygostylian *Confuciusornis* indicated by a preserved body profile, proposes the first upstroke-enhanced flight stroke. Slender ventral body profiles in the early-diverging birds *Archaeopteryx* and *Anchiornis* suggest habitual use of the pectoralis could not maintain the sternum through bone functional adaptations. Increased wing-assisted terrestrial locomotion potentially accelerated sternum loss through higher breathing requirements. Lower expected downstroke requirements in the early thermal soarer *Sapeornis* could have driven sternum loss through bone functional adaption, possibly encouraged by the higher breathing demands of a *Confuciusornis*-like upstroke. Both factors are supported by a slender ventral body profile. These data validate the ancestral shoulder/chest flight system and provide insights into novel upstroke-enhanced flight strokes and early sternum loss, filling important gaps in our understanding of the appearance of modern flight.

flight origins | feathered dinosaurs | early birds | preserved soft tissues | early flight stroke

Significance

Modern birds power their flight stroke using chest muscles. This evolved from an ancestral flight system thought to be divided between shoulder muscles powering the upstroke and chest muscles powering the downstroke. This is inferred from bony fossil anatomy and extant comparative anatomy, but validation from preserved soft anatomy has remained elusive. Here we reveal soft anatomy body profiles of the earliest theropod flyers preserved as residual skin chemistry covering the body and delimiting its margins. These data independently validate the ancestral shoulder/chest divided flight system, and allowed us to identify the first upstroke-enhanced flight stroke and explain early sternum losses. This study fills important gaps in our understanding of early paravian flight prior to the modern chest-driven flight system.

Ancestral paravian theropod dinosaurs developed flapping-based locomotion utilizing a range of anatomical features, thus setting the stage for flight to evolve. These features include smaller body size (1, 2), aerodynamic feathers (1, 3), elongated and robust forelimbs (1, 4), a laterally facing glenoid fossa, a laterally everted anterior edge of the acromion margin, and a symmetrical furcula (5). Evidence suggests that flight capabilities ranging from gliding through powered flight evolved among paravians multiple times (5–8). The potential for full weight-supporting, organism-driven flapping flight evolved at least once in birds and twice in dromaeosaurids (5). All early-diverging avialans seem to have the potential for true flapping flight except possibly *Xiaotingia* (5), with some appearing to have already evolved more specialized flight styles, such as thermal soaring (9). Many nonflying paravian taxa and their ancestors were in fact on the cusp of being flyers (5, 10). Beyond Paraves, membrane-winged scansoriopterygid theropods had the potential for gravity-driven gliding flight (11).

A range of approaches and lines of evidence have been used to reconstruct the powered flight capabilities of paravians. This includes functional morphology of flight-related anatomy, form–function relationships, first-principles–based modeling, morphologically informed morphospace analysis, interactive musculoskeletal modeling and simulation, as well as wind tunnel experiments using physical models (12). Previous work has capitalized on our understanding of modern birds, but this necessitates certain assumptions, including soft-tissue flight anatomy that is typically unknown in fossil specimens (12).

New fossils, combined with instrumentation and imaging, such as laser-stimulated fluorescence (LSF), have enabled us to accumulate observations of preserved paravian flight-related soft tissues, revising past assumptions, such as the shape and extent of the propatagium (13). As most wing motion takes place at the shoulder, this is a key target for observations of preserved soft-tissue flight anatomy. The chest region is also a key target because it hosts the upstroke and downstroke flight muscles in modern birds.

Author contributions: M.P., T.G.K., X.W., and X.Z. designed research; M.P., T.G.K., X.W., X.Z., T.A.D., and S.A.H. performed research; M.P., T.G.K., X.W., X.Z., and S.A.H. contributed new reagents/analytic tools; M.P., T.G.K., X.W., X.Z., T.A.D., and S.A.H. analyzed data; and M.P., T.G.K., X.W., X.Z., T.A.D., and S.A.H. wrote the paper.

The authors declare no competing interest.

This article is a PNAS Direct Submission. D.V. is a guest editor invited by the Editorial Board.

[1] To whom correspondence may be addressed. Email: mpittman@cuhk.edu.hk or wangxiaoli@lyu.edu.cn.

This article contains supporting information online at http://www.pnas.org/lookup/suppl/doi:10.1073/pnas.2205476119/-/DCSupplemental.

Published November 14, 2022.

Unfortunately, observation of preserved soft anatomy in both regions has been limited and elusive.

Here we document the preserved soft-tissue profiles of the shoulder and chest of early flying paravians, observed as residual skin chemistry covering the body and delimiting its margins, taken from a sample of over 1,000 fossil specimens. Soft-tissue identification was facilitated by LSF (13). We transpose these soft anatomy data onto quantitative skeletal reconstructions to make comparisons with the ancestral shoulder/chest divided flight system predicted by hard anatomy and comparisons with modern birds and crocodylians. We then discuss their implications for our understanding of early flight development in theropods.

Results and Discussion

Nonavialan Paravians. *Microraptor* is a small microraptorine dromaeosaurid with asymmetrical flight feathers on the wings and legs (14). Functional morphology and aerodynamic analysis through modeling and calculations demonstrates that *Microraptor* was the first paravian outside of birds (used here as equivalent to Avialae) that had the potential for gliding flight (7, 15–18). Recent first-principles modeling shows that *Microraptor* and another dromaeosaurid, *Rahonavis*, met the full weight support and climb-out requirements for true flapping flight (5). Outside of birds, *Microraptor* and *Rahonavis* are the only known paravians capable of this feat (5). These nonavialan flyers did not have a triosseal canal, but *Microraptor* did have a sternum (*Rahonavis* specimen UA 8656 and 100+ specimens of *Microraptor* observed). Existing musculoskeletal reconstructions of noncoelurosaurian and nonavialan paravian theropods utilizing extant comparative anatomy (19–28) suggest that the potentially anterodorsal–posteroventral wing movements of early nonavialan paravians (22, 23) featured the deltoids and supracoracoideus on the upstroke and the pectoralis on the downstroke (Fig. 1).

This flight system configuration in *Microraptor* is confirmed using LSF imaging, which identified a relatively large soft-tissue profile preserved around the deltopectoral crest (STM 5-221) and smaller one around the coracoid (IVPP V13352). This suggests that the deltoids and supracoracoideus muscles were relatively larger around the deltopectoral crest than the supracoracoideus around the coracoid (Fig. 2). *Microraptor* has a sternum that was fused, flat and wide (e.g., IVPP V13352, STM 5-93, and STM 5-142) and anchored a ventrally positioned pectoralis muscle that powered the downstroke (21). Delaminated sternal bone in specimen STM 5-93 reveals linearity in the internal bone texture that fans outward anteriorly toward the shoulder girdle (Fig. 2). This suggests directional bone functional adaptations relating to the habitual flight-related loading of the sternum (in the sense of ref. 29). In modern flying birds, the internal texture of the sternal plates tends be nonlinear (30). This probably relates to the predominant role of the keel, a feature that is absent in *Microraptor*. In contrast, the common ancestor of dromaeosaurids and their closest troodontid relatives probably had a sternum but was not a flyer.

Troodontids, the closest relatives of dromaeosaurids, have yet to be reconstructed with powered flight capabilities as their arms are too short despite their relatively small size (5). Troodontids had a less carnivorous diet indicated by their numerous stout teeth and generally shortened their forelimbs over evolutionary time (31). They also lacked a sternum. If their forelimb shortening was linked to a reduced need for prey handling associated with their dietary shift, it is possible that this was a driver of sternum loss. However, the closely related oviraptorosaurians had a less carnivorous diet but had sterna (31, 32), so the absence of the sternum in troodontids remains enigmatic.

Earliest Fossil Birds. The earliest-diverging birds were long-tailed and are traditionally thought to be powered flyers. Their flight capability was based on the functional morphology of their skeletons and feathering (33–39), as well as estimates of take-off (40), weight support (5, 10), climb-out capability (5, 10), wing bone geometry (41), and physical aerodynamic modeling (42, 43). Like nonavialan paravian flyers (this study), the earliest fossil birds controlled their potentially anterodorsal–posteroventral wing movements (22, 23, 41) with an ancestral theropod flight system. This is suggested by the absence of a triosseal canal and a reconstructed musculoskeletal arrangement similar to existing ones of nonavialan theropods (19–21, 28, 44). This ancestral theropod flight system featured the dorsally positioned deltoids and supracoracoideus controlling the upstroke and the ventrally positioned pectoralis controlling the downstroke (Fig. 1). A vestige of this ancestral system is present in modern birds that can use their deltoids for upstroke capacity (25–27) and can still fly when the supracoracoideus tendon is cut (27).

Unlike nonparavian theropods and dromaeosaurids, the earliest-diverging long-tailed avialans, *Archaeopteryx* and *Anchiornis* (but not the Jeholornithiformes), appear to lack a bony or cartilaginous sternum (45). LSF imaging of 8 specimens of *Archaeopteryx* (Berlin, Haarlem, Eichstätt, Solnhofen, Munich, Daiting, Thermopolis, and the 11th specimen) and 147 specimens of *Anchiornis* (STM 0-1 to 0-147) supports this absence. In particular, specimens that preserve cartilage (e.g., cartilaginous pubic callosity preserved in *Anchiornis* STM-0-118) were not found to preserve cartilaginous sternal plates. This evidence would seem to rule out cartilaginous sternal plates in at least these taxa (against ref. 46). Unlike the sternumless troodontids, both *Archaeopteryx* and *Anchiornis* have been reconstructed with powered flight potential (5, 41). However, this does not fully consider the missing sternum which seems counter-intuitive for a flyer. The sternum would be expected to recede and eventually be lost if its habitual loading regime (stress and strain) was significantly reduced compared to the sternum-bearing ancestral avialan (47). This suggests that the earliest long-tailed avialan flyers without a sternum exhibited a more limited downstroke capability. Our detection of a shallow ventral body contour in *Anchiornis* specimen STM 0-114 indicates a relatively slender pectoralis that supports this inference (Fig. 3). Additionally, becoming more cursorial and using both the legs and wings for locomotion may have imposed higher breathing demands that could have contributed to further release of the chest and sternum loss (also congruent with the body contour recovered). Increased gastralial aspiration would be evident from a higher gastralia count (48), as observed in the 13 to 14 pairs of gastralia estimated in *Anchiornis* (49) and 12 to 13 pairs reported in *Archaeopteryx* (50).

Short-Tailed Birds. The long tails of the earliest birds gave way to a shorter tail that led to the functional decoupling of the tail and wings, paving the way for new flight styles (9, 51, 52). These early pygostylians inherited the ancestral theropod flight system of the first birds that featured dorsally positioned upstroke muscles and ventrally positioned downstroke muscles (Fig. 1). Through the study of ∼600 confuciusornithid fossils, we infer a slender pectoralis associated with an unkeeled sternum based on the relatively small ventral soft-tissue profile observed in *Confuciusornis* STM 13-20 (Fig. 4). This validates the lesser role of the sternum in powered flight compared to modern birds (53) as well as the hypothesis that avialan sternal

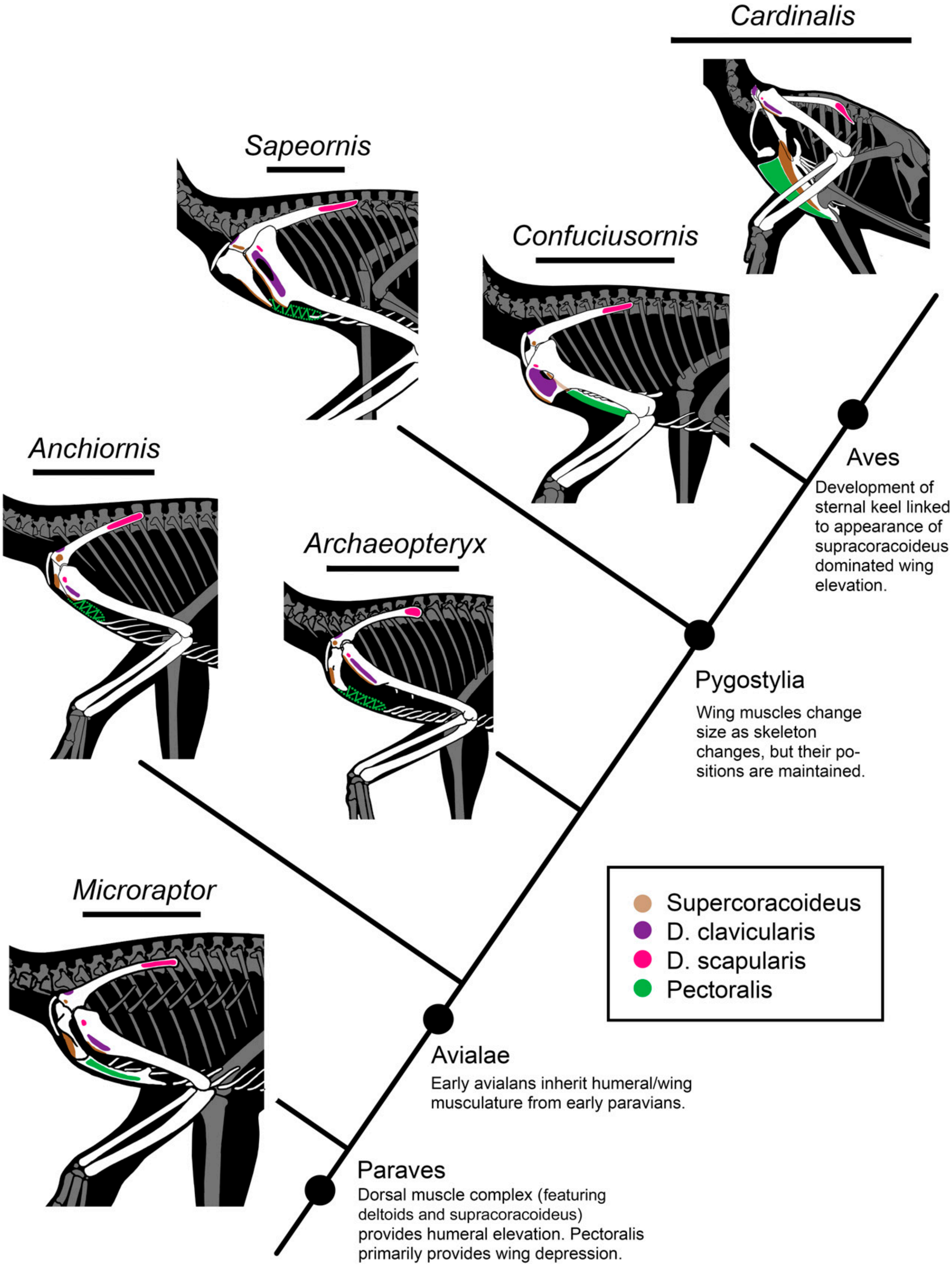

Fig. 1. Important flight muscles in flighted nonavialan paravians (*Microraptor*), early-diverging sternumless avialans (*Archaeopteryx* and *Anchiornis*) and early-diverging pygostylians with and without a sternum (*Confuciusornis* and *Sapeornis*, respectively). Musculoskeletal reconstructions of noncoelurosaurian and fossil paravian theropods utilizing extant comparative anatomy (19–23, 25–28) suggest that the potentially anterodorsal-posteroventral wing movements of early nonavialan paravians (22, 23) featured the deltoids and supracoracoideus on the upstroke and the pectoralis on the downstroke. Flight muscles only acquire their modern configuration (represented by the northern cardinal, *Cardinalis*) when the supracoracoideus extended onto the keeled sternum (54). Skeletal reconstructions with key bones in white (*Methods*). Muscle colors after Burch (19): purple for deltoideus clavicularis, pink for deltoideus scapularis, brown for supracoracoideus, and green for pectoralis. Cross-hatching indicates the inferred site of attachment in sternumless taxa. The exact attachment sites for the pectoralis in these taxa remain controversial, but is suspected to be on cartilaginous sternal plates (46) and anterior gastralia (49). Medial deltopectoral crest insertions of the pectoralis are hidden from view. (Scale bars, 5 cm.)

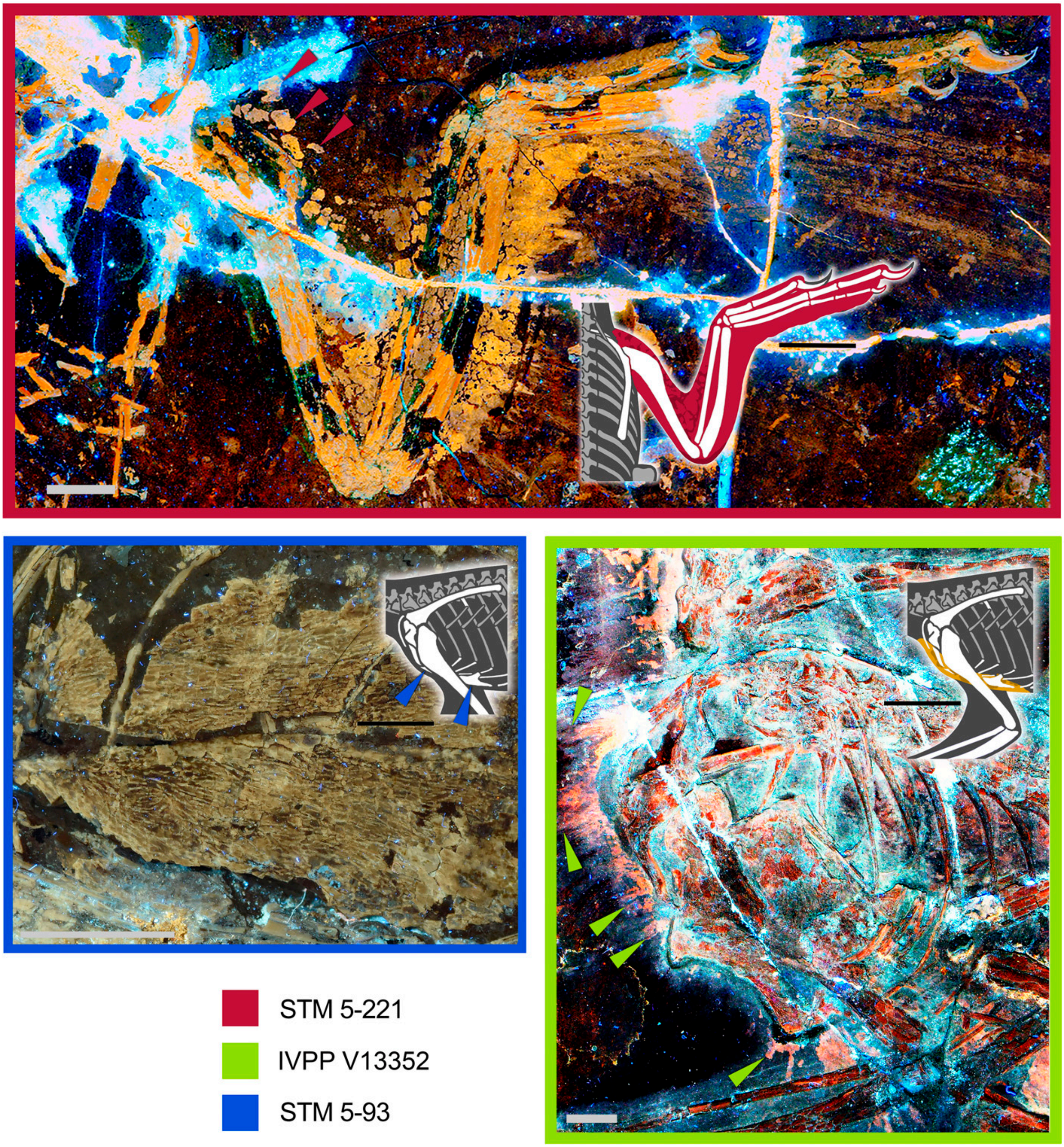

Fig. 2. Flight-related soft and hard anatomy in a nonavialan paravian exemplified by *Microraptor*. Clockwise from left: STM 5-221, soft-tissue profile of the wing and shoulder in yellow fluorescent color under LSF (outline marked with red arrows; also preserved in specimens STM 5-109 and 5-172). The soft tissues are preserved as a thin and fragile veneer on the specimen surface and appear to have a desiccated, cracked appearance. This is its superficial appearance as some of the preserved soft tissues are on the counterslab while minor missing portions have broken off from the slabs. The area of preserved soft tissues points to significant deltoid and supracoracoideus muscles surrounding the enlarged deltopectoral crest in life, supporting the upstroke. (Scale bar, 10 mm.) *Inset* shows preserved soft tissue anatomy transposed onto skeletal reconstruction. (Scale bar, 50 mm.) (*Lower Right*) IVPP V13352, slender chest profile in an orange fluorescent color under LSF suggests a relatively slender pectoralis muscle powering the downstroke. Outline marked with green arrows. (Scale bar, 10 mm.) *Inset* shows preserved soft tissue anatomy transposed onto skeletal reconstruction. (Scale bar, 50 mm.) (*Lower Left*) STM 5-93, delaminated sternum showing linearity in the internal bone structure associated with flight-related loading. (Scale bar, 10 mm.) *Inset* shows preserved soft-tissue anatomy transposed onto quantitative reconstruction. (Scale bar, 50 mm.)

keel development is linked to migration of the supracoracoideus onto the sternum (54) and the deepening of the pectoralis muscle.

Confuciusornis is known for its extremely enlarged deltopectoral crest that increased in size along the lineage (55). This large deltopectoral crest has been suggested as compensation for the lack of an elongate, keeled sternum (56). Our specimen survey ($n \sim 600$) yielded observations of a broad soft tissue profile preserved around the humerus of *Confuciusornis* (STM 13-292

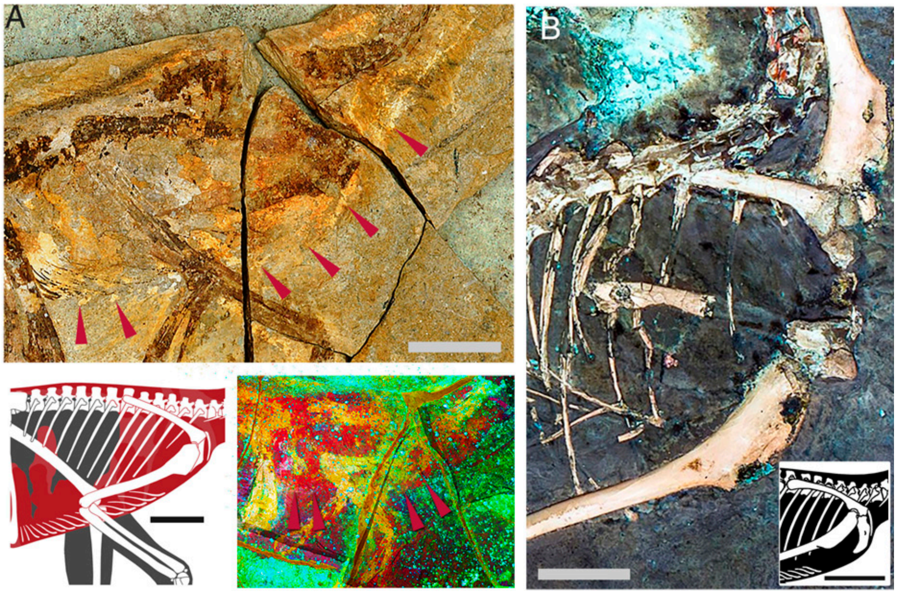

Fig. 3. Flight-related soft and hard anatomy of the earliest sternumless birds exemplified by *Anchiornis* and *Archaeopteryx*. (*A*) Body contours along the neck, chest and belly of the early long-tailed sternumless bird *Anchiornis* STM 0-1, including slender soft tissues around the relatively compact humeral deltopectoral crest. (Scale bar, 20 mm.) Outline marked by red arrows. *Inset* shows LSF image of specimen with outline marked by red arrows and skeletal reconstruction with transposed preserved soft tissues in red (*Methods*). (Scale bar, 50 mm.) (*B*) *Archaeopteryx* had a comparatively longer and more expansive humeral deltopectoral crest than *Anchiornis* so it should have a comparatively larger body contour, but its preserved shape is currently unknown. LSF image of the Berlin specimen of *Archaeopteryx* MB.Av.101. (Scale bar, 20 mm.) Skeletal reconstruction of *Archaeopteryx* (*Methods*), (Scale bar, 50 mm.)

and 13-54) (Fig. 4). This directly validates the large size of the deltoids and supracoracoideus predicted by the enlarged deltopectoral crest, and crucially shows its spatial extent (Fig. 4). Taken together with our observations of a slender sternal profile in *Confuciusornis*, our data suggests that it was powered by the ancestral shoulder/chest divided flight system with a heavily constructed shoulder and weakly constructed chest that evidences *Confuciusornis* as the first example of an upstroke-enhanced flight stroke. *Confuciusornis* is also unique in preserving an incipient propatagial ligament along the leading edge of the wing, the earliest record of this ligament to our knowledge (STM 13-44) (Fig. 4). Thus, we can also infer that *Confuciusornis* maintained leading edge tautness to improve its aerodynamics and minimize aeroelastic flutter (57).

The early pygostylian *Sapeornis* is proposed as a thermal soarer (9, 58). This lifestyle can potentially explain its lack of a sternum (45) (confirmed through LSF imaging of 106 fossil specimens) because rising thermals provide lift to thermal soarers during flight so they are less dependent on the downstroke for lift (9). This would reduce sternal loading leading to sternum loss through bone functional adaptation. As another early pygostylian with an especially enlarged deltopectoral crest, *Sapeornis* may also have had a *Confuciusornis*-like upstroke-enhanced flight stroke. This is also indicated by its relatively small ventral body contour observed under LSF (STM 15-15 in Fig. 4). The completely preserved gastralia series of *Sapeornis* is one of the longest of any early-diverging bird (49) and is expected to have enhanced its capacity for gastralial aspiration (48). This improved breathing function presumably enhanced the flight capacity of *Sapeornis*. *Sapeornis* has been thought to lack a triosseal canal, although an incipient feature has been proposed (54, 59), but the supracoracoideus is unlikely to have been a strong depressor in this taxon as we did not observe a relatively large respective body contour but only a relatively small one (STM 15-15 in Fig. 4). Our validation of the ancestral theropod flight system and insights into sternum loss and novel upstroke-enhanced flight strokes fill important gaps in our understanding of early flight prior to the appearance of the modern chest-powered flight stroke.

Methods

LSF Imaging of Preserved Skeleton and Soft Tissues. LSF imaging is based on the original protocol of Kaye et al. (60). A 0.5 W 405-nm laser diode was used to fluoresce the fossil specimens according to standard laser safety protocol. Thirty-second time-exposed images were taken with a Nikon D810 DSLR camera fitted with a 425-nm laser-blocking filter. Postprocessing was applied uniformly across entire images (equalization, saturation and color balance) in graphics software *Photoshop CS6*.

Experimental Validation of Preserved Soft-Tissue Outline. A confined compression experiment was designed and performed to determine if the soft-tissue profiles preserved were the result of body deformation. An apparatus consisting of a 4-inch-diameter vertical steel tube with a removable aluminum plug base was partially filled with calcium carbonate powder (micrite) and tamped flat. Newborn bird wings were placed on this partial fill. Wings were specifically chosen as part of the experimental design due to their large variation in thickness and shape to maximize the chances of detecting body deformation during compression. The chicken wing had a size magnitude difference of ∼10 with the thinnest portion being the ∼1-mm leading edge of the propatagium and the thickest portion being the ∼10-mm-thick shoulder joint. The duck wing was of more uniform thickness, ∼5-mm thick. More calcium carbonate powder was then used to completely cover the wing surface to a depth of at least 2 cm. A second aluminum plug was fitted on top of the vertical tube to seal it, completely containing the specimen and its surrounding matrix. This plug-matrix-plug assembly was placed in a hydraulic press and compressed with 8 tons of pressure for 12 h. *SI Appendix*, Fig. S1 shows the wings before and after compression. The confined compression experiment shows that the outlines were similar before and after compression, even with the ∼10 magnitude-sized difference in the chicken wing's thickness. These results provide high confidence in our analysis of the soft tissues preserved. The thorax is the widest and heaviest part of feathered dinosaurs. Thus, this region potentially has the most chance of showing shape deformation in the soft-tissue preserving fossils analyzed in this study. This was typically not the case. In the example shown in *SI Appendix*, Fig. S2, a laterally compressed thorax of the early bird *Anchiornis* has the ribs in place and

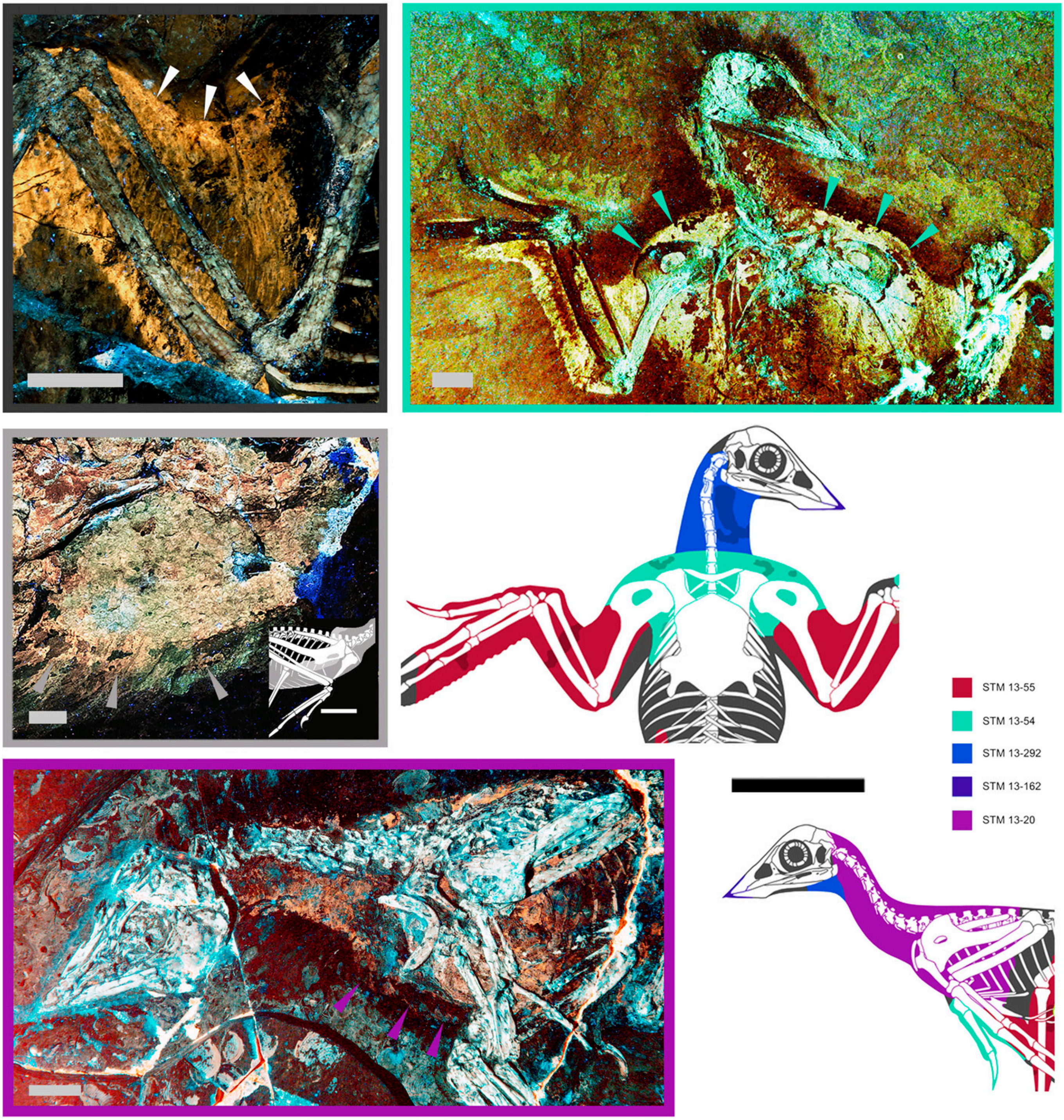

Fig. 4. Flight-related soft tissue and bone anatomy of an early pygostylian bird as exemplified by *Confuciusornis*. The broad shoulder and slim chest profiles of the early pygostylian bird *Confuciusorni*s suggest that it had extraordinarily large deltoid and supracoracoideus muscles originating from the humerus, but a relatively slender pectoralis hosted by the unkeeled sternum. Preserved soft tissues were transposed onto a ventral and lateral skeletal reconstruction based on a survey of ~600 specimens, with ~300 revealing preserved soft tissues under LSF (13) (*Methods*). (Scale bar, 50 mm.) (*Top Left*) Predecessor of the propatagial ligament along the leading edge of the wing in STM 13-44 (marked by red arrows). (*Top Right*) STM 13-54 preserves soft tissue profiles around the deltopectoral crest and of the propatagium (outline marked by green arrows). (*Bottom Left*) STM 13-20 preserves a relatively small ventral body profile suggesting there was a slender pectoralis muscle associated the unkeeled sternum also seen in STM 13-12 (outline marked with purple arrows). (Scale bars, 10 mm.) (*Middle*) Relatively small ventral profile of the early pygostylian *Sapeornis* STM 15-15 under LSF. (Scale bar, 10 mm.) *Inset* shows preserved soft tissues transposed onto a skeletal reconstruction. (Scale bar, 50 mm.) These data indicate that a slender pectoralis was associated with the sternumless chest (*Methods*).

the overlying skin remains within its natural outline, which is also indicated by a regular pattern of preserved feather follicles (*SI Appendix*, Fig. S2).

Skeletal Reconstruction. The skeletons were reconstructed using Adobe Photoshop CC versions 2015–2021. Individual bones were scaled from high-resolution photographs with minimal parallax using the Ruler Tool in Photoshop. Virtual scaling was done from literature values, when possible, and set according to scale bars using Photoshop's Custom Scaling tool otherwise. The following specimens were used for the skeletal reconstructions in Figs. 1–4: *Microraptor*: IVPP V13352; *Anchiornis*: primarily STM 0-118, with missing caudal elements cross-scaled from STM 0-114; *Archaeopteryx*: primarily WDC CSG 100, with cervical and mandibular elements cross-scaled from HMN 1880/81; *Confuciusornis*: the lateral aspect skeletal is restored after STM 13-20, while the ventral aspect skeletal is based on STM 13-54; *Sapeornis*: primarily IVPP V13276, with cervical and select pectoral girdle elements from IVPP V13276, and cranial anatomy clarified via STM 16-18; *Cardinalis*: UWZS 38948. Other articulated and well-exposed early-diverging paravians and contemporary biomechanics work [including published interpretations of theropod limb kinematics (52, 61)] was also used to help reconstruct vertebral curvature and pose the skeleton, including rib and shoulder girdle orientation. Major elements were illustrated on separate layers to facilitate rotation and transformation into plausible life positions.

Transposition of Preserved Soft Tissues onto Skeletal Reconstructions. Based on the validation experiment, pristine soft tissues were taken at face value and transposed quantitatively onto respective skeletal reconstructions. Fragmentary missing soft tissues were marked in an off color. No specimens were used that had obvious taphonomic issues: for example, soft-tissue dislocation from the bones, soft-tissue desiccation, and differential soft-tissue degradation. Minor remaining unpreserved portions of the body outlines were based on dissections of birds and published myology (62, 63) and marked in black in Figs. 1–4. To accommodate soft-tissue data from specimens of differing size, tissue depth was measured as a percentage of bone width or length. We assigned anatomical terms for soft tissues based on the observed morphology (e.g., bones, body contours and propatagium).

Data, Materials, and Software Availability. All study data are included in the main text and *SI Appendix*.

ACKNOWLEDGMENTS. We thank attendees of the inaugural International Pennaraptoran Dinosaur Symposium held in Hong Kong in 2018 and authors of the journal volume *Pennaraptoran Theropod Dinosaurs: Past Progress and New Frontiers* for their input and feedback. This study was supported by the Research Grant Council of Hong Kong's General Research Fund (17103315; 17120920; 17105221), the Taishan Scholars Program of Shandong Province (Ts20190954), and the Faculty of Science & School of Life Sciences of The Chinese University of Hong Kong.

Author affiliations: [a]School of Life Sciences, The Chinese University of Hong Kong, Hong Kong Special Administrative Region, China; [b]Foundation for Scientific Advancement, Sierra Vista, AZ 85650; [c]Institute of Geology and Paleontology, Linyi University, Shandong 276005, China; [d]Shandong Tianyu Museum of Nature, Shandong 273300, China; [e]Division of Natural Sciences, Mount Marty University, Yankton, SD 57078; and [f]Department of Integrative Biology, University of Wisconsin–Madison, Madison, WI 53706-1692

1. X. Xu *et al.*, An integrative approach to understanding bird origins. *Science* **346**, 1253293 (2014).
2. A. H. Turner, D. Pol, J. A. Clarke, G. M. Erickson, M. A. Norell, A basal dromaeosaurid and size evolution preceding avian flight. *Science* **317**, 1378–1381 (2007).
3. X. Xu *et al.*, Mosaic evolution in an asymmetrically feathered troodontid dinosaur with transitional features. *Nat. Commun.* **8**, 14972 (2017).
4. X. Xu, H. You, K. Du, F. Han, An *Archaeopteryx*-like theropod from China and the origin of Avialae. *Nature* **475**, 465–470 (2011).
5. R. Pei *et al.*, Potential for powered flight neared by most close avialan relatives, but few crossed its thresholds. *Curr. Biol.* **30**, 4033–4046.e8 (2020).
6. S. Hartman *et al.*, A new paravian dinosaur from the Late Jurassic of North America supports a late acquisition of avian flight. *PeerJ* **7**, e7247 (2019).
7. S. Chatterjee, R. J. Templin, Biplane wing planform and flight performance of the feathered dinosaur *Microraptor gui. Proc. Natl. Acad. Sci. U.S.A.* **104**, 1576–1580 (2007).
8. P. J. Makovicky, S. Apesteguía, F. L. Agnolín, The earliest dromaeosaurid theropod from South America. *Nature* **437**, 1007–1011 (2005).
9. F. J. Serrano *et al.*, "Laser-stimulated fluorescence refines flight modelling of the early cretaceous bird sapeornis" in *Pennaraptoran Dinosaurs: Past Progress and New Frontiers*, M. Pittman, X. Xu, Eds. (American Museum of Natural History, New York, 2020), pp. 333–344.
10. T. A. Dececchi, H. C. E. Larsson, M. Pittman, M. B. Habib, "High flyer or high fashion? A comparison of flight potential among small-bodied paravians" in *Pennaraptoran Theropod Dinosaurs: Past Progress and New Frontiers*, M. Pittman, X. Xu, Eds. (American Museum of Natural History, New York, 2020) pp. 295–320.
11. T. A. Dececchi *et al.*, Aerodynamics show membrane-winged theropods were a poor gliding dead-end. *iScience* **23**, 101574 (2020).
12. M. Pittman *et al.*, "Methods of studying early theropod flight" in *Pennaraptoran Theropod Dinosaurs: Past Progress and New Frontiers*, M. Pittman, X. Xu, Eds. (American Museum of Natural History, New York, 2020), pp. 277–294.
13. X. Wang *et al.*, Basal paravian functional anatomy illuminated by high-detail body outline. *Nat. Commun.* **8**, 14576 (2017).
14. X. Xu *et al.*, Four-winged dinosaurs from China. *Nature* **421**, 335–340 (2003).
15. G. Dyke *et al.*, Aerodynamic performance of the feathered dinosaur *Microraptor* and the evolution of feathered flight. *Nat. Commun.* **4**, 2489 (2013).
16. C. Palmer, The aerodynamics of gliding flight and its application to the arboreal flight of the Chinese feathered dinosaur *Microraptor. Biol. J. Linn. Soc. Lond.* **113**, 828–835 (2014).
17. D. Evangelista *et al.*, Aerodynamic characteristics of a feathered dinosaur measured using physical models. Effects of form on static stability and control effectiveness. *PLoS One* **9**, e85203 (2014).
18. D. E. Alexander, E. Gong, L. D. Martin, D. A. Burnham, A. R. Falk, Model tests of gliding with different hindwing configurations in the four-winged dromaeosaurid *Microraptor gui. Proc. Natl. Acad. Sci. U.S.A.* **107**, 2972–2976 (2010).
19. S. H. Burch, Myology of the forelimb of *Majungasaurus crenatissimus* (Theropoda, Abelisauridae) and the morphological consequences of extreme limb reduction. *J. Anat.* **231**, 515–531 (2017).
20. S. H. Burch, Complete forelimb myology of the basal theropod dinosaur *Tawa hallae* based on a novel robust muscle reconstruction method. *J. Anat.* **225**, 271–297 (2014).
21. S. C. Jasinoski, A. P. Russell, P. J. Currie, An integrative phylogenetic and extrapolatory approach to the reconstruction of dromaeosaur (Theropoda: Eumaniraptora) shoulder musculature. *Zool. J. Linn. Soc.* **146**, 301–344 (2006).
22. F. E. Novas *et al.*, Comments on the morphology of basal paravian shoulder girdle: New data based on unenlagiid theropods and paleognath birds. *Front. Earth Sci.* **9**, 662167 (2021).
23. F. E. Novas, F. L. Agnolín, F. Brisson Egli, G. E. Lo Coco, "Pectoral girdle morphology in early-diverging paravians and living ratites: Implications for the origin of flight" in *Pennaraptoran Theropod Dinosaurs: Past Progress and New Frontiers*, M. Pittman, X. Xu, Eds. (American Museum of Natural History, New York, 2020), pp. 345–353.
24. S. H. Hwang, M. A. Norell, Q. Ji, K. Q. Gao, New specimens of *Microraptor zhaoianus* (Theropoda: Dromaeosauridae) from Northeastern China. *Am. Mus. Novit.* **3381**, 1–44 (2002).
25. K. P. Dial, G. E. Goslow Jr., F. A. Jenkins Jr., The functional anatomy of the shoulder in the European starling (*Sturnus vulgaris*). *J. Morphol.* **207**, 327–344 (1991).
26. R. A. Meyers, Gliding flight in the American Kestrel (Falco sparverius): An electromyographic study. *J. Morphol.* **215**, 213–224 (1993).
27. L. A. Degernes, A. Feduccia, Tenectomy of the supracoracoideus muscle to deflight pigeons (*Columba livia*) and cockatiels (*Nymphicus hollandicus*). *J. Avian Med. Surg.* **15**, 10–16 (2001).
28. G. E. Goslow, K. P. Dial, F. A. Jenkins, The avian shoulder: An experimental approach. *Am. Zool.* **29**, 287–301 (1989).
29. M. Wong, D. R. Carter, Mechanical stress and morphogenetic endochondral ossification of the sternum. *J. Bone Joint Surg. Am.* **70**, 992–1000 (1988).
30. O. P. Choudhary *et al.*, Gross morphological studies on the sternum of crested serpent eagle (*Spilornis cheela*). *Indian J. Anim. Res.* **52**, 1459–1461 (2019).
31. P. J. Makovicky, M. A. Norell, "Troodontidae" in *The Dinosauria*, D. B. Weishampel, P. Dodson, H. Osmólska, Eds. (University of California Press, Berkeley, 2004), pp. 184–209.
32. W. Ma, M. Pittman, R. J. Butler, S. Lautenschlager, Macroevolutionary trends in theropod dinosaur feeding mechanics. *Curr. Biol.* **32**, 677–686.e3 (2022).
33. P. Wellnhofer, *Archaeopteryx–The Icon of Evolution* (Verlag Dr. Friedrich Pfeil, München, 2009).
34. N. R. Longrich, J. Vinther, Q. Meng, Q. Li, A. P. Russell, Primitive wing feather arrangement in *Archaeopteryx lithographica* and *Anchiornis huxleyi. Curr. Biol.* **22**, 2262–2267 (2012).
35. R. L. Nudds, G. J. Dyke, Narrow primary feather rachises in *Confuciusornis* and *Archaeopteryx* suggest poor flight ability. *Science* **328**, 887–889 (2010).
36. R. Å. Norberg, Feather asymmetry in *Archaeopteryx. Nature* **374**, 221–222 (1995).
37. A. Feduccia, H. B. Tordoff, Feathers of *archaeopteryx*: Asymmetric vanes indicate aerodynamic function. *Science* **203**, 1021–1022 (1979).
38. D. W. Yalden, C. D. Bramwell, W. B. Heptonstall, Flying ability of Archaeopteryx. *Nature* **231**, 127–128 (1971).
39. D. B. O. Savile, The primaries of *Archaeopteryx. Auk* **74**, 99–101 (1957).
40. P. Burgers, L. M. Chiappe, The wing of *Archaeopteryx* as a primary thrust generator. *Nature* **399**, 60–62 (1999).
41. D. F. A. E. Voeten *et al.*, Wing bone geometry reveals active flight in *Archaeopteryx. Nat. Commun.* **9**, 923 (2018).
42. J. Meseguer *et al.*, Lift devices in the flight of *Archaeopteryx. Spanish Journal of Paleontology* **27**, 125–130 (2012).
43. A. M. Heers, K. P. Dial, B. W. Tobalske, From baby birds to feathered dinosaurs: Incipient wings and the evolution of flight. *Paleobiology* **40**, 459–476 (2014).
44. S. L. Olson, A. Feduccia, Flight capability and the pectoral girdle of *Archaeopteryx. Science* **278**, 247–248 (1979).
45. X. Zheng *et al.*, On the absence of sternal elements in *Anchiornis* (Paraves) and *Sapeornis* (Aves) and the complex early evolution of the avian sternum. *Proc. Natl. Acad. Sci. U.S.A.* **111**, 13900–13905 (2014).
46. W. J. Bock, The furcula and the evolution of avian flight. *Paleontol. J.* **47**, 1236–1244 (2013).
47. O. M. Pearson, D. E. Lieberman, The aging of Wolff's "law": Ontogeny and responses to mechanical loading in cortical bone. *Am. J. Phys. Anthropol.* **125** (suppl. 39), 63–99 (2004).
48. L. P. A. M. Claessens, Dinosaur gastralia; origin, morphology, and function. *J. Vertebr. Paleontol.* **24**, 89–106 (2004).
49. J. M. K. O'Connor, X. T. Zheng, X. L. Wang, X. M. Zhang, Z. H. Zhou, The gastral basket in basal birds and their close relatives: Size and possible function. *Vertebrata Palasiatica* **53**, 133–152 (2015).
50. A. Elzanowski, "Archaeopterygidae (Upper Jurassic of Germany)" in *Mesozoic Birds: Above the Heads of Dinosaurs*, L. M. Chiappe, L. M. Witmer, Eds. (University of California Press, Berkeley, 2002), pp. 129–159.
51. M. Pittman, S. M. Gatesy, P. Upchurch, A. Goswami, J. R. Hutchinson, Shake a tail feather: The evolution of the theropod tail into a stiff aerodynamic surface. *PLoS One* **8**, e63115 (2013).
52. S. M. Gatesy, "Locomotor evolution of the line to modern birds" in *Mesozoic Birds: Above the Heads of Dinosaurs*, L. M. Chiappe, L. M. Witmer, Eds. (University of Berkeley Press, Berkeley, 2002), pp. 432–447.
53. T. M. Lowi-Merri, R. B. J. Benson, S. Claramunt, D. C. Evans, The relationship between sternum variation and mode of locomotion in birds. *BMC Biol.* **19**, 165 (2021).
54. G. Mayr, Pectoral girdle morphology of Mesozoic birds and the evolution of the avian supracoracoideus muscle. *J. Ornithol.* **158**, 859–867 (2017).
55. G. Navalón *et al.*, Diversity and evolution of Confuciusornithidae: Evidence from a new 131-million-year-old specimen from the Huajiying Formation in NE China. *J. Asian Earth Sci.* **152**, 12–22 (2018).

56. Z. Zhou, F. Z. Li, Z. Li, A new Lower Cretaceous bird from China and tooth reduction in early avian evolution. *Proc. Biol. Sci.* **277**, 219–227 (2010).
57. C. J. Pennycuick, *Modelling the Flying Bird* (Academic Press, London, 2008).
58. F. J. Serrano, L. M. Chiappe, Aerodynamic modelling of a Cretaceous bird reveals thermal soaring during avian evolution. *J. R. Soc. Interface* **14**, 20170182 (2017).
59. S. Wang *et al.*, Digital restoration of the pectoral girdles of two Early Cretaceous birds and implications for early-flight evolution. *eLife* **11**, e76086 (2022).
60. T. G. Kaye *et al.*, Laser-stimulated fluorescence in paleontology. *PLoS One* **10**, e0125923 (2015).
61. J. R. Hutchinson, V. Allen, The evolutionary continuum of limb function from early theropods to birds. *Naturwissenschaften* **96**, 423–448 (2009).
62. J. J. Baumel, Ed., *Handbook of Avian Anatomy: Nomina Anatomica Avium* (Nuttall Ornithological Club, Cambridge, ed. 2, 1993), **vol. 23**.
63. J. R. Hutchinson, K. T. Bates, V. Allen, *Tyrannosaurus rex* redux: *Tyrannosaurus* tail portrayals. *Anat. Rec. (Hoboken)* **294**, 756–758 (2011).